AIR FORCE ACADEMY

Multidisciplinary Optimisation of an Unmanned Aerial Vehicle With a Fuel Cell Powered Energy System

Bernardo Miguel Teixeira Alves
ALF/ENGAER 139425-J

Abstract

To explore the use of hydrogen fuel cells as a feasible alternative to pollutant fuels on Unmanned Aerial Vehicles (UAVs), a class I concept was designed at the Portuguese Air Force Research Centre. This work focuses on the trade-off studies performed during its design and on the optimisation that followed. First, a multi-objective optimisation approach was used with the aid of the Algorithm NSGA-II to balance between two conflicting objectives: low weight and high endurance. It was found that it is possible to fly for more than 3 hours with a Maximum Take-off Weight of 21.6 kg, an 800 W fuel cell and 148 g of hydrogen. A heavier configuration with more power and fuel was discarded due to a wingspan constraint. Later, after the concept satisfied the project requirements, Multi-Disciplinary Design Optimisation (MDO) was performed to achieve the maximum endurance possible. The software used was OpenAeroStruct, low fidelity Finite Element Analysis (FEA) and Vortex Lattice Method (VLM) to model lifting surfaces. Initially, a cruise and a load flight point were used with wing geometric twist only as design variable. After, more complexity was added by introducing taper, wing chord and span. Finally, a third flight point was introduced to ensure the stall requirements were satisfied. The use of MDO allowed a 21% increase in endurance with a smaller wing area. Other improvements could not be achieved without violation of the constraints. This work marks an important milestone in the development of a future prototype at the Research Centre.

Keywords: MDO, UAV, Green Aircraft, Multi-objective optimisation, eVTOL, Conceptual Design

1 Introduction

The use of hydrogen as an alternative to fossil fuels is of interest to the defense sector. It is considered key for reaching the European Union goal of carbon neutrality and sustainability (Edwards, Kuznetsov, David, & Brandon, 2008; European Union, 2020). It then becomes useful to explore ways of using H_2 in the different sectors of society. One possible use of this molecule would be to power Unmanned Aerial Vehicles (UAVs).

Since 2009, with the PITVANT project (Morgado & Sousa, 2009), the Portuguese Air Force has developed and tested UAS and thus acquired valuable know-how and experience in both the design and later in the operation of class I vehicles. With the intent of exploring the application of fuel cells on UAVs and acquire knowledge in the field of renewable energies, a project to design, build and later test an UAS prototype begun at the Portuguese Air Force Research Centre (CIAFA).

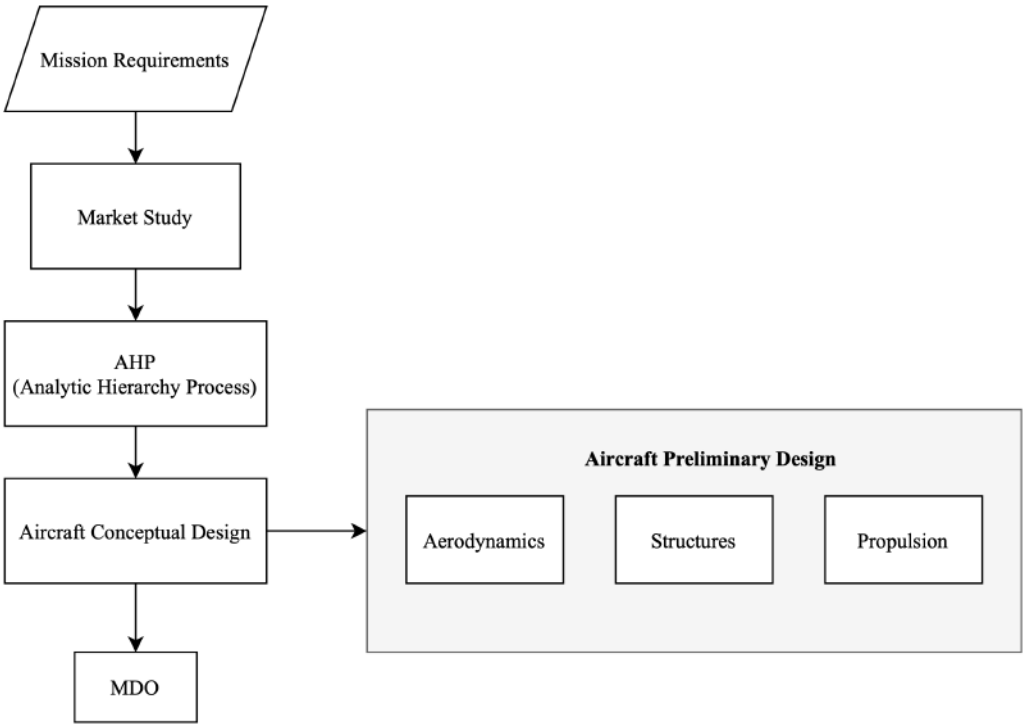

Figure 1: Project flowchart

Table 1: Design proposal presented by CIAFA

Requirement	Value	Description
MTOM	$<$ 25 kg	-
Payload	2 kg	Includes a daylight camera
Endurance	$>$ 2 h	Preferable over 3 hours
Cruise Speed	35-45 kts	-
Stall Speed	$<$ 25 kts	Without Flaps
Maximum Speed	70 kts	-
Ceiling	15 000 ft	Mean Sea Level
Takeoff & Landing	-	VTOL, fully autonomous
Maximum Takeoff Altitude	10 000 ft	Above Mean Sea Level
Engine Type	-	Electric

A representative flowchart is provided in Figure 1. It started with a given set of requirements, which can be found in

Table 1. Afterwards, an Analytic Hierarchy process was performed to select the most suitable configuration with respect to a set of defined criteria. Then, the conceptual design of the UAV was carried with help of a numerical program. At this stage, two distinct works began: the preliminary design of the UAV (Coelho, 2021; P. Silva, 2021; Sá, 2021) and multi-disciplinary-optimisation of the proposed concept.

This work focuses on the trade-off studies that were done in the conceptual phase, to help decide which fuel cell and hydrogen tank would be best suited for the defined mission profile; and on the multi-disciplinary optimisation of the baseline model that followed. Trade-off studies allowed to assess the impact of Maximum Take-Off Weight (MTOW) on endurance. To achieve a desired compromise between the two, some adjustments to the project requirements were made. The use of MDO allowed a quick and effective search of the design space to improve upon the proposed model.

2 Methods

2.1 Multi-Objective Optimisation

To perform the trade-off studies during the design of the UAV a numerical program developed by the author together with P.Silva, Sá, and Coelho was used (Alves et al., 2021). It uses a methodology based on Gundlach (2014) to estimate both endurance and MTOW for a given mission profile, which must be defined by the user. Other outputs of the program are the size of the motors, rotors, wing and batteries. Due to the iterative nature of the solver implemented, a stopping criteria was defined: an absolute tolerance of 1 gram, and, as fallback, a maximum of 50 iterations were allowed.

This tool was coupled with the Elitist Non-dominated Sorting Genetic Algorithm II (NSGA-II) (Deb, Pratap, Agarwal, & Meyarivan, 2002), available in the Pymoo framework (Blank & Deb, 2020), to solve multi-objective optimisation problems with respect to both endurance and MTOW. The NSGA-II is a real-coded genetic algorithm that uses the non-dominated sorting and crowded-distance comparison operators to form the Pareto-front with the best solutions possible. These operators are applied to the parent and offspring populations, thus elitism is enforced. The search for improvement from one generation to the next is achieved with traditional GA operators like selection, crossover and mutation (Goldberg, 1989).

2.2 A Multi-Disciplinary Approach to Aircraft Design

OpenAeroStruct (Jasa, Hwang, & Martins, 2018) was used to perform the multi-disciplinary design optimisation of the baseline wing. OpenAeroStruct is a low fidelity tool, which uses the Vortex-Lattice Method (VLM) to determine the aerodynamic forces acting on the lifting surfaces; and Finite-Element Analysis (FEA) to calculate stresses and displacements. It was developed on top of NASA's OpenMDAO framework (Gray, Hwang, Martins, Moore, & Naylor, 2019), whose responsibility is to converge the aerostructural model and calculate its total derivatives to allow the correct functionality of the gradient-based optimisers.

OpenMDAO provides a modular environment to facilitate the integration of the different disciplines, each is defined as an implicit function which is later used in the unified derivatives equation to determine the derivatives of the coupled model, this approach is the Modular-Analysis and Unified Derivatives (MAUD) (Hwang & Martins, 2018). With this framework, the main responsibility of the end-user is to define each individual component and provide the partial derivatives of the outputs with respect to the inputs. This framework also provides features that simplify the connection of the coupling variables between different components. In practise, this allows the end-user to easily define his/her own models, make the necessary connections to analyse it and perform optimisation with the aid of gradient-based optimisers.

OpenAeroStruct uses the Vortex-Lattice-Method to evaluate the aerodynamic loads that act on the lifting surface, as illustrated in Figure 2. VLM models each lifting surface as thin plate subjected to a horseshoe vortex system. Each vortex filament induces a velocity at an arbitrary point P, as given by the Bio-Savart Law,

$$d\boldsymbol{V} = \frac{\Gamma}{4\pi} \cdot \frac{d\boldsymbol{l} \times \boldsymbol{r}}{|\boldsymbol{r}|^3}, \tag{1}$$

where Γ represents the circulation strength, r the distance between the vortex and P where the flow field is being assessed,

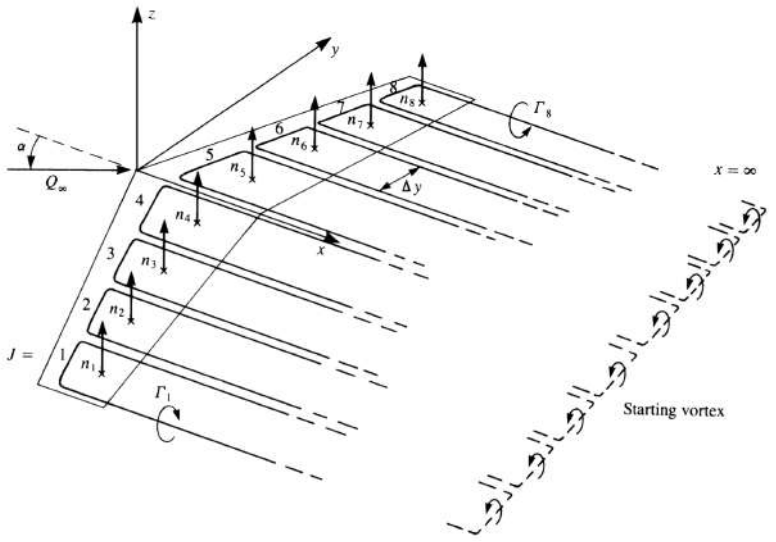

Figure 2: Illustrative VLM model with multiple horseshoe vortices along the span, retrieved from Katz and Plotkin (2001)

and $d\boldsymbol{l}$ is the length of the vortex filament. Integration over a semi-infinite straight vortex yields

$$V = \frac{\Gamma}{4\pi h}, \tag{2}$$

with h being the distance between P and the start point of the vortex filament. After establishing the relation between the strength of the vortex and the induced speed, the flow tangency condition is enforced at all the control points of each horseshoe vortex. This results in a system of linear equations of the form

$$\boldsymbol{A\Gamma} = -\boldsymbol{V}_\infty \cdot \boldsymbol{n}, \tag{3}$$

where A is the aerodynamic influence coefficient matrix and $\boldsymbol{V}_\infty$ represents the non-disturbed flow field. By solving this system, $\boldsymbol{\Gamma}$ is found. Then, the aerodynamic forces acting on each panel can be calculated using

$$\boldsymbol{F}_i = \rho\Gamma_i \left(\boldsymbol{V}_\infty + \boldsymbol{v}_i\right) \times \boldsymbol{l}_i. \tag{4}$$

Decomposing them in the direction of free-stream and its perpendicular, drag and lift are estimated.

The structural model consists of a spatial beam-bar element with six degrees of freedom per node. The stiffness matrix for a single element is

$$[k]_e = \begin{bmatrix}
k_1 & 0 & 0 & 0 & 0 & 0 & -k_1 & 0 & 0 & 0 & 0 & 0 \\
0 & 12k_2^z & 0 & 0 & 0 & 6k_2^z l & 0 & -12k_2^z & 0 & 0 & 0 & 6k_2^z l \\
0 & 0 & 12k_2^y & 0 & -6k_2^y l & 0 & 0 & 0 & -12k_2^y & 0 & -6k_2^y l & 0 \\
0 & 0 & 0 & k_3 & 0 & 0 & 0 & 0 & 0 & -k_3 & 0 & 0 \\
0 & 0 & -6k_2^y l & 0 & 4k_2^y l^2 & 0 & 0 & 0 & 6k_2^y l & 0 & 2k_2^y l^2 & 0 \\
0 & 6k_2^z l & 0 & 0 & 0 & 4k_2^z l^2 & 0 & -6k_2^z l & 0 & 0 & 0 & 2k_2^z l^2 \\
-k_1 & 0 & 0 & 0 & 0 & 0 & k_1 & 0 & 0 & 0 & 0 & 0 \\
0 & -12k_2^z & 0 & 0 & 0 & -6k_2^z l & 0 & 12k_2^z & 0 & 0 & 0 & -6k_2^z l \\
0 & 0 & -12k_2^y & 0 & 6k_2^y l & 0 & 0 & 0 & 12k_2^y & 0 & 6k_2^y l & 0 \\
0 & 0 & 0 & -k_3 & 0 & 0 & 0 & 0 & 0 & k_3 & 0 & 0 \\
0 & 0 & -6k_2^y l & 0 & 2k_2^y l^2 & 0 & 0 & 0 & 6k_2^y l & 0 & 4k_2^y l^2 & 0 \\
0 & 6k_2^z l & 0 & 0 & 0 & 2k_2^z l^2 & 0 & -6k_2^z l & 0 & 0 & 0 & 4k_2^z l^2
\end{bmatrix} \tag{5}$$

After the assembly of the global stiffness matrix $\boldsymbol{K}$, the linear system of equations

$$\boldsymbol{Ku} = \boldsymbol{f} \tag{6}$$

is solved. For OpenAeroStruct to determine the stiffness matrix for each element, its cross-sectional properties, such as

the second moment of area and the polar moment of inertia are necessary. These are calculated using a wingbox model, which allows the use of the spar and skin thicknesses as design variables during the optimisation problem. Nevertheless, the distance between the front and rear spars are defined based on the airfoil coordinates that were inserted by the user. Along the wingspan, these coordinates are scaled with the local chord but the relative distance between then, e.g front spar at 10% and rear spar at 60%, cannot change. Furthermore, it is not possible to use different airfoils in OpenAeroStruct. There are other parameters that can be used as design variables, for reference consult Chauhan and Martins (2019).

To couple the aerostructural model, it is necessary to transfer the aerodynamic loads to the structures to determine the displacements and stresses. Then, the new aerodynamic loads must be found for the deformed shape of the wing, and the process repeats until convergence occurs

$$\boldsymbol{\mathcal{R}}_i(\boldsymbol{y}, \boldsymbol{y}^t) = 0, \tag{7}$$

i.e, when the target $\boldsymbol{y}^t$ and state $\boldsymbol{y}$ variables match. Different solvers in OpenMDAO can be used to find the solution. After it has been found, the objective function and constraints of the optimisation problem can be evaluated.

The load transfer scheme implemented in OpenAeroStrcut is both consistent and conservative, (Jasa et al., 2018). This process is simplified by using the same span wise discretisation for both the FEM elements and the VLM panels. Finally, in the wingbox model used, the location of the shear centre is also needed. Its position is estimated based on an average of the location of the spars, weighted by their respective area (Chauhan & Martins, 2019).

The baseline UAV has electric motors, which are powered by a hydrogen fuel cell. Hence, the variation in weight is negligible when compared to the MTOW. The endurance equation from Raymer (1992),

$$E = \frac{L}{D} \frac{E_{sb}\ \eta_{b2s}\ \eta_p}{(W_0 + W_s)\ V}\ m_b, \tag{8}$$

was added to the Functional Evaluations of OpenAeroStruct. First, an OpenMDAO ExplicitComponent was defined. The definition of the partial derivatives of endurance with respect to each input was done using analytic methods. Then, this component was instantiated inside the *total_perf*, which is an OpenMDAO Group. Some of the parameters which were assumed constant during the optimisation process are stored inside *prob_vars* component.

OpenAeroStruct has several geometric manipulation functions that can be used to define the initial shape of the lifting surface and to modify it during optimisation. One of such functions is the *Taper*, which can be used to decrease the chord linearly from the root until the tip. To use it, the user must define the ratio $\lambda = c_{tip}/c_{root}$. By default, transformation happens around the quarter-chord line.

A new taper function was sought to decrease the chord linearly from a user-defined position until the tip while keeping the leading-edge perpendicular to the fuselage. A bottom-up approach was used. First, a new OpenMDAO ExplicitComponent was created: the user-defined inputs are the ratio λ, and an offset which must be given as a percentage of the semi-span. The output is the altered mesh. Secondly, analytic partial derivatives of the output (mesh) with respect to the inputs (taper and offset) were defined. For simplicity, it was assumed that the derivative of the mesh with respect to the offset would be zero, hence this parameter cannot be used as design variable. The necessary connections between components were made and this new geometric manipulation function tested. This new development in OpenAeroStruct allows an easier definition of general trapezoidal lifting-surfaces and also the use of λ as design variable in the optimisation problem, without affecting the rectangular portion of the wing.

3 Results

3.1 Conceptual Aircraft Design Using Multi-Objective Optimisation

During the conceptual phase of the project, a lift+cruise configuration was selected based on an analytic hierarchy process (AHP) (Saaty & Vargas, 2012) with a set of defined criteria. The pusher configuration was chosen together with an inverted V tail. The later is connected to the fuselage by a double boom.

The typical mission profile starts with a vertical take-off, which is accomplished with the an independent propulsive system powered by Li-Po batteries. After, transition between vertical and conventional mode occurs. To perform the transition

between these two, the horizontal propeller is turned on and the vertical flight rotors are shut down. The conventional mode is powered by a fuel cell that converts stored hydrogen in the tank to electric current. In this flight mode, the UAV will climb, surveil a desired area or target and return back to the starting point. It will land vertically, with the rotors although it can also land in conventional mode, if desired. A representative mission profile is shown in Figure 3.

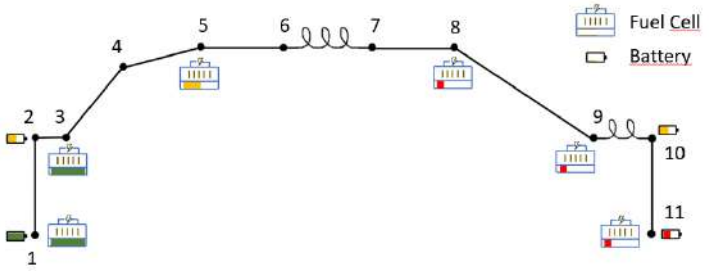

Figure 3: Main mission profile, retrieved from Alves et al. (2021)

Some important parameters had to be estimated at this stage, refer to Alves et al. (2021, sec. 5) for a complete list. The multi-objective optimisation problem is posed in standard form

$$\begin{aligned} \text{Minimise/Maximise} \quad & f_m(\boldsymbol{x}), && m = 1, 2, ..., M; \\ \text{subject to} \quad & g_j(\boldsymbol{x}) \leq 0, && j = 1, 2, ..., J; \\ & h_k(\boldsymbol{x}) = 0, && k = 1, 2, ..., K; \\ & x_i^L \leq x_i \leq x_i^U, && i = 1, 2, ..., n. \end{aligned} \tag{9}$$

where $\boldsymbol{f}$ can be written in vector form as

$$\boldsymbol{f}(\boldsymbol{x}) = \begin{Bmatrix} MTOW(\boldsymbol{x}) \\ -Endurance(\boldsymbol{x}) \end{Bmatrix} \begin{bmatrix} \text{kg} \\ \text{Hours} \end{bmatrix}, \tag{10}$$

with MTOW being the sum of the structural weight, related to the airframe; propulsion system weight, which takes the motors, ESC and propeller/rotors into account; energy weight, which accounts for batteries and hydrogen; other weights to account for cables, servos, avionics, the hydrogen tank and the payload

$$MTOW(x) = W_s + W_{prop.system} + W_{energy} + W_{other} \quad \text{[kg]} \tag{11}$$

and Endurance is the sum of the time needed to accomplish each mission segment,

$$Endurance(x) = \sum_{i=1}^{N} t_i \quad \text{[h]} \tag{12}$$

where i represents the mission segment and N the total number of segments. To ensure the design requirements were met, the inequality constraints

$$\boldsymbol{g}(\boldsymbol{x}) = \begin{Bmatrix} MTOW(\boldsymbol{x}) - 25 \\ -E(\boldsymbol{x}) + 2.5 \\ b(\boldsymbol{x}) - 4.0 \\ P_{\text{Con. Mode}} - P_{\text{nominal}} \\ m_{\text{fuel}} - m_{\text{tank}} \\ V_{\text{stall}} - V_{\text{Op}} + 8 \end{Bmatrix} \begin{bmatrix} kg \\ h \\ m \\ W \\ g \\ kts \end{bmatrix} \leq 0 \tag{13}$$

were added to the problem: g_1 sets the maximum MTOW; g_2 sets the minimum endurance time; g_3 limits the maximum wingspan; g_4 ensures the maximum power needed in conventional mode is lower than the fuel cell nominal power; g_5 ensures the amount of fuel needed is within tank capacity; and g_6 establishes that the minimum operational speed is at

least 8 kts above stall.

Table 2: Design variables for the multi-objective optimisation problem.

Design var.	Description	Lower bound	Upper bound	Units
x_1	Disk loading, W/A	100	350	N/m^2
x_2	Wing loading, W/S	100	250	N/m^2
x_3	Wing aspect ratio	5	12	-
x_4	Loiter time	2	∞	h
x_5	Stall speed	26	32	kts
x_6	Operational speed	30	45	kts

A total of six design variables were used, being their description and bounds provided in Table 2.

With the numerical program developed and the Pymoo multi-objective optimisation framework mentioned in Section 2, some experiments were done to define a suitable convergence criteria to find a compromise between accuracy and cost. A tolerance of 10^-3 was used for both the constraints and the objective space, in addition a tolerance of $5 \cdot 10^{-4}$ was set to the design space. As fallback, the number of maximum generation was set to 150.

Initially, the multi-objective problem was solved with the requirements defined in Table 1 and the first four design variables of Table 2, but no feasible solution was found. The causes of such result were investigated and it was concluded that either the stall speed or the wingspan constraint had to be relaxed. The decision makers opted for relaxing the stall speed motivated by the fact that the UAV would have a VTOL system.

After solving the same optimisation problem with the relaxed stall speed, $V_{stall} = 30$ kts, a Pareto-front was obtained. After comparing several solutions from the front it was concluded that although the g_4 constraint was satisfied, the margin between the maximum power required to the fuel cell system and its actual nominal power was low (refer to Alves et al. (2021) for details).

Because the estimation of the base drag coefficient C_{D_0} had some uncertainty associated with it, other solutions with higher power margins were to be sought. To increase the power margin two possibilities were assessed: in the first, the fuel cell was upgraded to increase the nominal power; in the second, some performance in conventional mode was sacrificed to decrease the maximum power needed.

Another parameter with high uncertainty is the estimated weight of the hydrogen tank, since it was estimated with a constant ratio and the required amount of hydrogen. Therefore, this estimate is replaced with commercially available tanks.

An upgrade on the fuel cell implies an upgrade to the hydrogen tank as well, due to the increase in weight and loss of efficiency in the cruise and loiter segments. So, two problems were formulated: one with a fuel cell with 800 W of nominal power and a tank with capacity for 148 g of H_2; and a fuel cell with 1300 W of nominal power and capacity for 175 g of H_2. In the first problem two additional design variables were added, x_5 and x_6 in Table 2. Since in both problems the tank is fixed, the constraint g_5 is added with $m_{\text{tank}} = 148$ and $m_{\text{tank}} = 175$ g, for the 800 W and 1300 W fuel cells, respectively. The convergence criteria remains unchanged. A superposition of the obtained Pareto-fronts is given in Figure 4.

All the solutions obtained with the lighter configuration, in orange, are better than the ones obtained with the heavier, in blue. Therefore, the 800 W fuel cell and the smaller tank were chosen. Due to the high specific energy of hydrogen, the total endurance time is extremely sensitive to the weight. As such, the tank will be completely full at take-off. The power consumption in each segment of the mission profile was analysed and suitable motors, propellers and batteries were selected in P. Silva (2021). The final characteristics of this concept can be found in (Alves et al., 2021, sec. 7). Finally, Coelho (2021) proposed a wing and tail for the concept.

3.2 Next Generation UAV Design

The main mission of the proposed concept is surveillance, hence maximisation of endurance Eq.(8) was sought. The product $E_{sb} \cdot m_b$ was replaced by the available energy content of 3479.85 W.h, which was estimated during the conceptual phase.

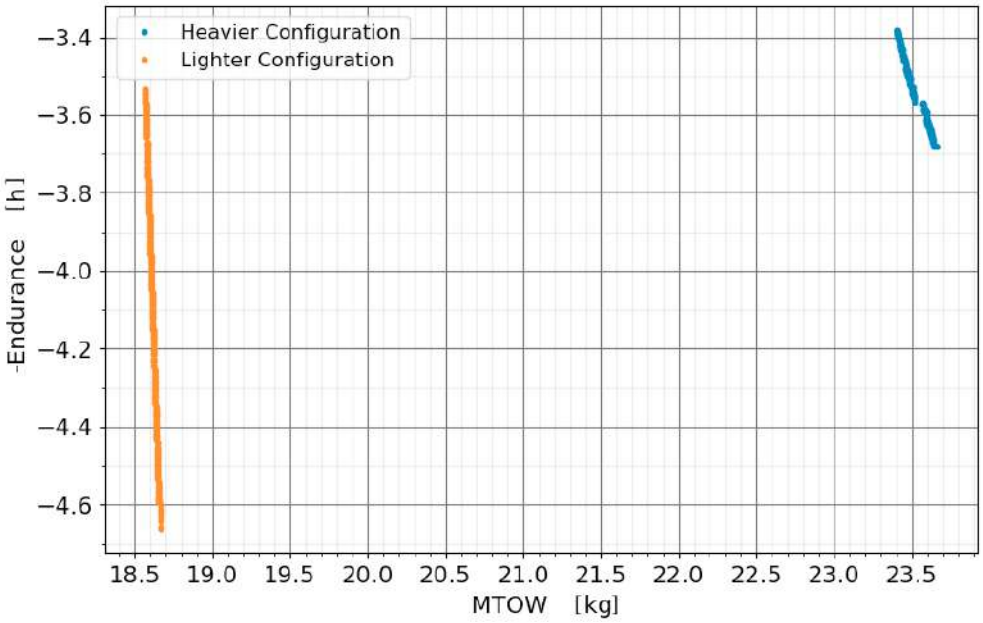

Figure 4: Comparison of the two different sets of Pareto-optimal solutions

Initially, the aerostructural problem was comprised of two distinct flight points. One corresponding to main surveillance mission, and another for a 6.0 g load case. The objective function would be maximised for the first condition and the wing structure would be sized for the second. Two lifting surfaces were defined: a wing and a tail. Both made of the same material, a composite made from a mixture of epoxy and bi carbon fibre (J. Silva, 2017). The structures were modelled as simplified wingboxes, with the front spar at 10% of the chord and the rear at 60%. The shape of each box was based on the coordinates of the selected airfoils: SG 6042 (Giguère & Selig, 1998) for the wing and NACA 008 for the tail. These properties are listed in Table 3.

Table 3: Parameters and specifications of the baseline UAV

Parameter	Value	Notes
Tank capacity	148 g of H_2	Maximum hydrogen stored
Energy	3479.85 W.h	Total energy available for main mission
MTOW	21.6 kg	
Main mission Mach	0.05647	
Main mission altitude	5000 ft	ISA + 20º C
6.0 g manoeuvre Mach.	0.07331	According to UAV's flight envelope
6.0 g manoeuvre altitude	0 ft	ISA + 20º C
Drag counts for VTOL rotors	350	
Aircraft weight without wing and tail structures	17.118 kg	
Structural material density	1300 kg/m^3	Based on epoxy + bi carbon fibre
Structural Young's modulus	48.99 MPa	Based on epoxy + bi carbon fibre
Structural shear modulus	5 GPa	Based on epoxy + bi carbon fibre
Structural yield strength	567.79 MPa	Based on epoxy + bi carbon fibre

To ensure that the UAV is in trimmed level flight, the constraints $L = W$ and $C_M = 0$ were added to the main mission. In the manoeuvre case, only the former was imposed. In this condition, a failure constraint based on the von Mises stresses aggregated with a Kreisselmeier–Steinhauser (KS) function (Kreisselmeier & Steinhauser, 1979) must also be satisfied. Finally, a monotonic constraint was added to ensure the optimiser introduces wash-out.

The design variables of the optimisation problem are: the wing geometric twist, spar and skin thicknesses, which are parametrised using b-splines; the angle of attack of the manoeuvre and main mission cases, and the tail incidence angle, which are scalars. The lower and upper bounds for the wing twist, spar and skin thicknesses are -15º and 15º, 0.6 and 3 mm, respectively. A summary of the optimisation problem is given in Table 4.

Table 4: Optimisation problem

	Function/variable	Note	Quantity
maximise	endurance	computed using Eq.(8)	
with respect to	wing twist	b-spline parametrised using 5 control points	5
	spar thickness	b-spline parametrised using 6 control points	6
	skin thickness	b-spline parametrised using 6 control points	6
	α	for the main mission	1
	α_i	for the main mission	1
	$\alpha_{\text{6.0 g}}$	for the 6.0 g load case	1
		Total design variables	**20**
subject to	$L = W$	for the main mission	1
	$C_M = 0$	in the main mission to ensure trimmed flight	1
	$L_{\text{6.0 g}} = W_{\text{6.0 g}}$	for the 6.0 g manoeuvre flight point	1
	$\sigma_{\text{von Mises}} \leq \frac{\sigma_{\text{yield}}}{2}$	von Mises stresses aggregated using a KS function	1
	$TA_{\text{monotonic}} < 0$	monotonic twist constraint	1
		Total constraint functions	**5**

The algorithm chosen is the SLSQP (Sequential Least Sqaures Programming) (Kraft, 1988) available in the Python library *SciPy* (Virtanen et al., 2020), with a tolerance of 10^{-7} and 200 maximum iterations as fallback.

To find a compromise between convergence of the solution and computational time, aerodynamic analysis of both lifting surfaces was done. The number of panels varied and L/D was observed. The compromise was set with 200 panels on half-wing, each section with 5 chord-wise nodes.

Afterwards, aerostructural analysis of the baseline UAV was done. Instead of allowing all the design variables to change, only $\alpha, \alpha_{\text{6.0 g}}$ and α_i were free so that trimmed level flight was possible. For a cruise speed of 38 kts, the obtained endurance of the baseline was 03h29 h:min with 21.6 kg of MTOW. The speed was kept fixed during all subsequent optimisations.

3.2.1 Optimisation With Geometric Twist

With the optimisation problem defined in Table 4 and the termination criteria defined, the program was executed. After 16 iterations, a solution had been found, while satisfying all constraints. The obtained parameter distributions along the wingspan and tailspan are shown in Figure 5.

Since twist was a design variable, the introduction of wash-out was expected to reduce the lift-induced drag and, as a consequence, maximise L/D to increase the endurance, as given by Eq.(8).

The obtained endurance was not significantly higher than the baseline, it improved 0.03%. Also, it was verified that the optimal solution had a worse aerodynamic efficiency when compared to the baseline. Still, endurance was better since the weight of the structures decreased enough. In fact, W_s is the lowest possible in this problem formulation, since both structural design variables correspond to the lower bounds. The reduction in weight and the low angle of attack suggested that flying with speeds lower than the defined 38 kts might increase the endurance of the vehicle. Because the speed was to be fixed, planform design variables were introduced in the problem.

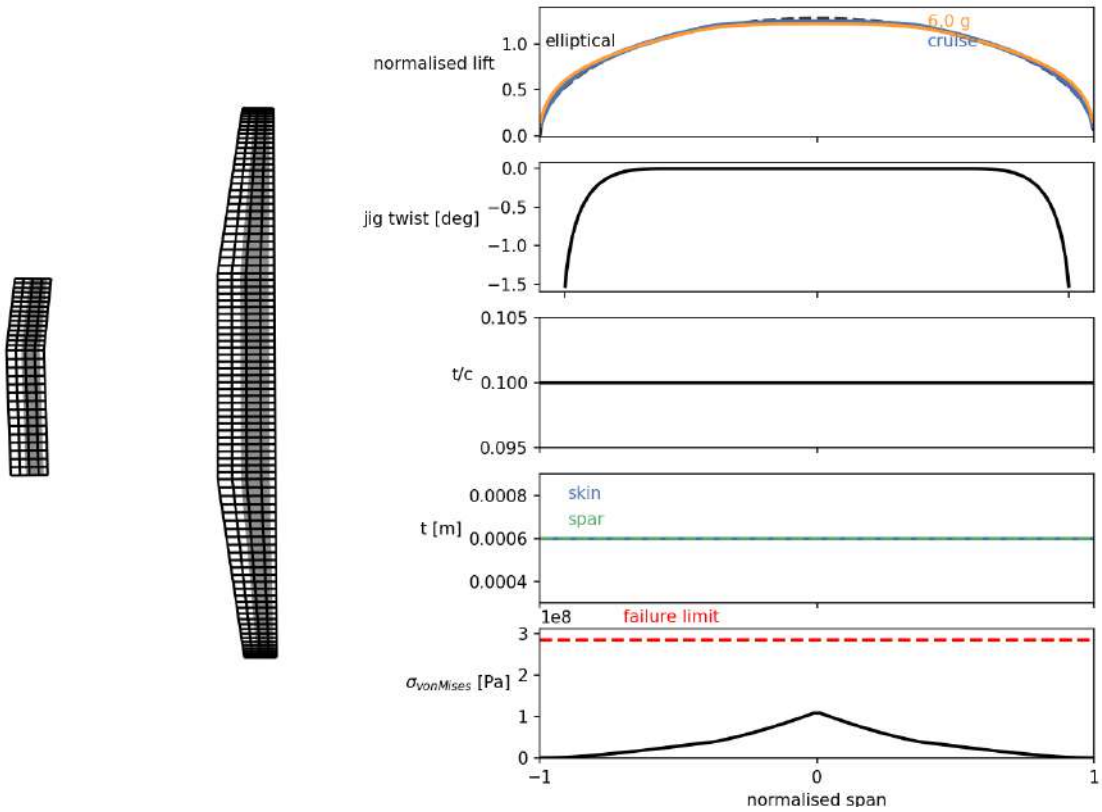

(a) Wing

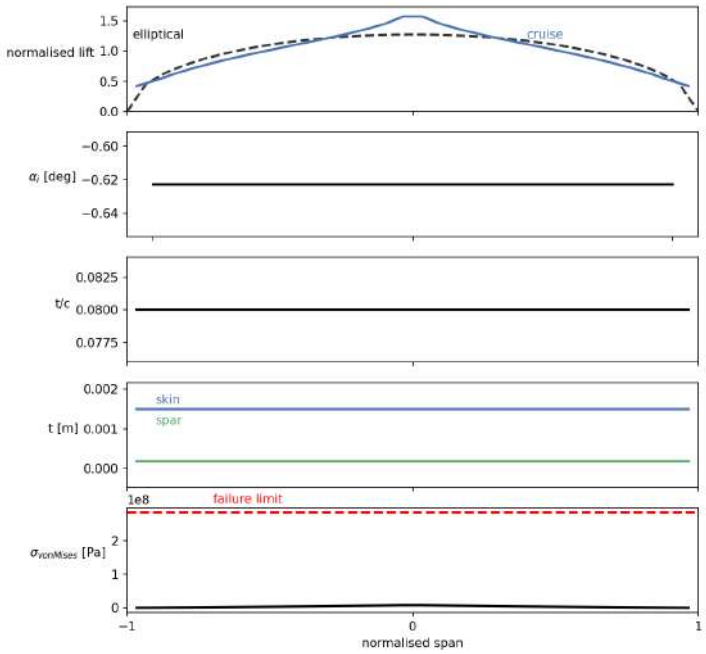

(b) Tail

Figure 5: Optimised parameter distribution along wingspan

3.2.2 Optimisation With Taper, Chord at Root and Wingspan

Using the wing twist as the only design variable was not enough to improve the performance of the baseline UAV. Furthermore, from a manufacturing point of view, it would be easier to construct a wing with adequate taper than a straight

wing with variable twist. The optimisation problem was solved with taper instead of twist as design variable and the results were analysed. Then, freedom was given to the chord at the wing root, and finally to the span. With each optimisation, some common trends were observed: for smaller wings, L/D was higher and W_s was lower, which maximises the endurance as given by Eq.(8); the reduction of the wing was being constrained by the upper bound of α, which was set at 10.0 deg.

At this point, a stall condition for the main mission was imposed. It was verified that the constraint was active for two of the optimal solutions found previously. Its effect on the new solutions can be observed in Figure 6.

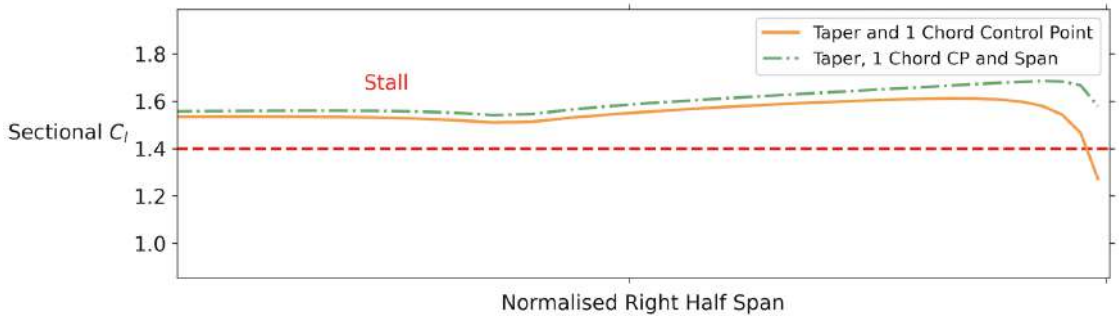

(a) Sectional lift coefficients without stall constraint

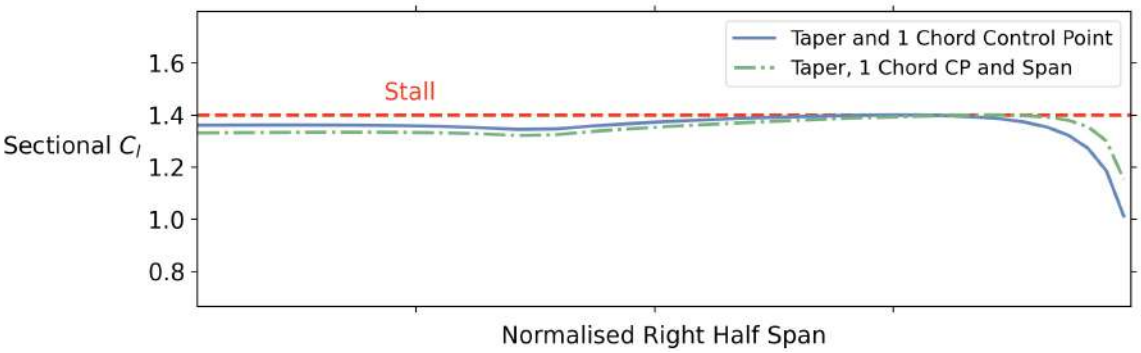

(b) Sectional lift coefficient with active stall constraint

Figure 6: Sectional lift coefficients along wingspan

3.2.3 Final Optimal Solution

With the previous optimal solutions, the UAV would perform the main surveillance mission near stall, which is unacceptable. Therefore, a third flight point was introduced in the OpenAeroStruct model to ensure the UAV would have a stall speed equal or lower than 28 kts. It is similar to the main mission, but it has a lower speed, which was set to 28 kts. An optimal solution was found after 25 iterations.

The same trends were observed. There was a reduction of the wing area, which was accomplished with $\lambda = 0.44$, $c_{root} = 0.272\,m$ and an increase in the wingspan. Consequently, L/D was higher and W_s was lower, which resulted in longer endurance times when compared to the baseline. However, the existence of the stall speed constraint did not allow the optimiser to reduce the wing area as much compared to when the stall constraint was inputed at cruise speed, and the estimated endurance was lower. Still, it was possible to increase the endurance up to 21% while satisfying all constraints.

A table with a summary of the results obtained in each of the mentioned solutions is provided in Table 5. The optimal parameter distribution along the wingspan and tailspan can be observed in Figure 7.

Table 5: Comparison between optimal solutions

	with twist		with planform design variables		with three flight cases	
Parameter	Value	Unit	Value	Unit	Value	Unit
Endurance	03:35	h:min	05:20	h:min	04:14	h:min
C_L	0.536	-	0.814	-	0.630	-
C_D	0.041	-	0.043	-	0.041	-
L/D	13.1	-	19.0	-	15.2	-
MTOW	19.4	kg	19.0	kg	19.0	kg
W_s	2.8	kg	2.36	kg	2.41	kg
α	2.4	deg	8.0	deg	3.9	deg
$\alpha_{6.0g}$	10.6	deg	20.1	deg	12.6	deg
α_i	-0.8	deg	-3.6	deg	-1.5	deg
c_{root}	0.399	m	0.186	m	0.272	m
λ	0.55	-	0.25	-	0.44	-
Span	4.0	m	4.9	m	4.7	m
S_{wing}	1.373	m^2	0.696	m^2	1.057	m^2

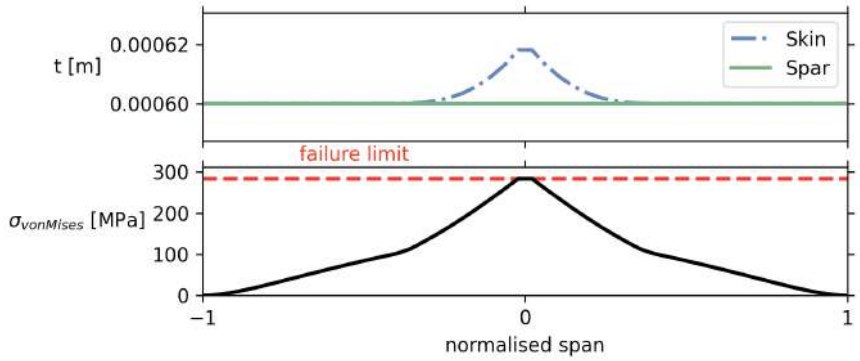

(a) Wing

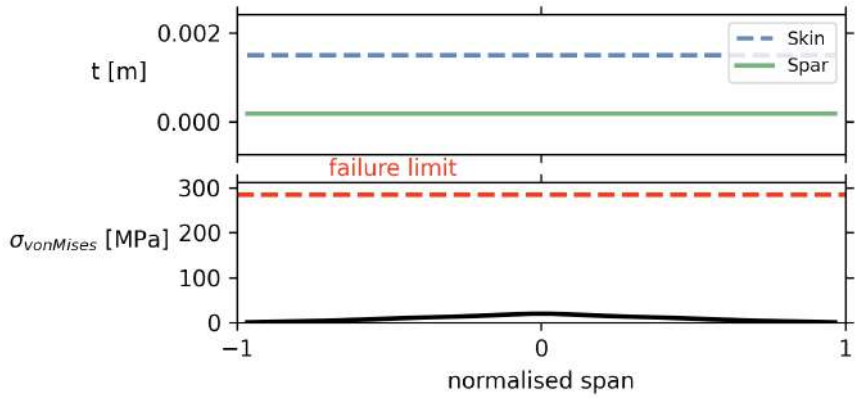

(b) Tail

Figure 7: Optimised parameter distribution obtained with three flight points

4 Conclusion

The first achievement of this work was the the sizing of a small UAV for surveillance operations in the Portuguese Air Force, refer to Section 3.1. This was accomplished in the early conceptual phase of the project by using an in-house developed software to estimate the vehicle's MTOW and endurance, together with a suitable *Open Source* framework to solve multi-objective optimisation problems. Doing so in the early stages of the project allowed to estimate the impact of some general design decisions on both objectives (weight and endurance), which contributed to a more informed decision process and to the adjustment of the project requirements.

Next, some developments with OpenAeroStruct were made to allow a definition of general planform shapes and to enable the estimation of the endurance for electric propeller driven aircraft. To improve the computational efficiency of the optimisation process, analytic partial derivatives were defined for these new components.

Afterwards, with the mentioned code developments, it was possible to search for improvements to the current baseline model, which had been designed during the conceptual phase of the project. The optimisation problem gradually grew in complexity. First, only twist was used as aerodynamic design variable, with no significant improvements obtained. Then, the wing twist was set to 0 deg and, instead, taper was used with different offsets. After the trends had been analysed, the chord at the inboard section of the wing and later the span are also allowed to change. With the optimisation results of these cases, some important trends were observed: wing area was being reduced and the aspect ratio was being increased. The lack of a stall constraint allowed to optimiser to take advantage of the problem formulation. This resulted in configurations that were flying with $\alpha = 10.0^o$ to ensure equilibrium, which was not possible. Therefore, the optimisation problem was re-formulated to take stall into account. For some solutions, the constraint was active in cruise and the optimiser increased the wing size to satisfy it.

Finally, to enforce the stall speed requirement, a third flight point was added with the equilibrium and stall constraints and no loads applied for level flight at 28 kts. From this optimisation, a smaller wing with a higher span was obtained which resulted in a 21% increase in the expected endurance of the UAV when compared to the baseline. Other solutions with extended endurance times were found but they do not satisfy this constraint.

References

Alves, B., Coelho, V., Silva, P., Marta, A., Afonso, F., Sá, P., ... Caetano, J. (2021, July). Design of a hydrogen powered small electric fixed-wing uav with vtol capability. In A. C. Marta & A. Suleman (Eds.), *International conference on multidisciplinary design optimization of aerospace systems* (p. 290-304). Lisbon, Portugal: IDMEC, IST. (ISBN: 978-989-99424-8-6)

Blank, J., & Deb, K. (2020). Pymoo: Multi-objective optimization in python. *IEEE Access*, *8*, 89497-89509.

Chauhan, S. S., & Martins, J. R. R. A. (2019). Low-fidelity aerostructural optimization of aircraft wings with a simplified wingbox model using openaerostruct. In H. Rodrigues et al. (Eds.), *Engopt 2018 proceedings of the 6th international conference on engineering optimization* (pp. 418–431). Cham: Springer International Publishing.

Coelho, V. (2021). *Aerodynamic detailed design of an unmanned aerial vehicle with a fuel cell powered energy system* (Unpublished master's thesis). Academia da Força Aérea, Sintra, Portugal.

Deb, K., Pratap, A., Agarwal, S., & Meyarivan, T. (2002). A fast and elitist multiobjective genetic algorithm: Nsga-ii. *IEEE Transactions on Evolutionary Computation*, *6*(2), 182-197. doi: 10.1109/4235.996017

Edwards, P., Kuznetsov, V., David, W., & Brandon, N. (2008). Hydrogen and fuel cells: Towards a sustainable energy future. *Energy Policy*, *36*(12), 4356-4362. (Foresight Sustainable Energy Management and the Built Environment Project) doi: 10.1016/j.enpol.2008.09.036

European Union. (2020, March). *Long-term low greenhouse gas emission development strategy of the european union and its member states.* Retrieved November 7, 2021, from `https://unfccc.int/documents/210328`

Giguère, P., & Selig, M. S. (1998). New Airfoils for Small Horizontal Axis Wind Turbines. *Journal of Solar Energy Engineering*, *120*(2), 108-114. doi: 10.1115/1.2888052

Goldberg, D. E. (1989). *Genetic algorithms in search, optimization and machine learning* (1st ed.). USA: Addison-Wesley Longman Publishing Co., Inc. doi: 10.1023/A:1022602019183

Gray, J. S., Hwang, J. T., Martins, J. R. R. A., Moore, K. T., & Naylor, B. A. (2019). OpenMDAO: An open-source framework for multidisciplinary design, analysis, and optimization. *Structural and Multidisciplinary Optimization*, *59*(4), 1075–1104. doi: 10.1007/s00158-019-02211-z

Gundlach, J. (2014). *Designing unmanned aircraft systems: A comprehensive approach, second edition*. American Institute of Aeronautics and Astronautics. doi: 10.2514/4.102615

Hwang, J. T., & Martins, J. R. R. A. (2018). A computational architecture for coupling heterogeneous numerical models and computing coupled derivatives. *ACM Transactions on Mathematical Software*, *44*, Article 37. doi: 10.1145/3182393

Jasa, J. P., Hwang, J. T., & Martins, J. R. R. A. (2018). Open-source coupled aerostructural optimization using python. *Structural and Multidisciplinary Optimization*, *57*(4), 1815-1827. doi: 10.1007/s00158-018-1912-8

Katz, J., & Plotkin, A. (2001). *Low-speed aerodynamics* (Vol. 13). Cambridge university press.

Kraft, D. (1988, July). *A software package for sequential quadratic programming* (Tech. Rep. No. DFVLR-FB 88-28). Koln, Germany: DLR German Aerospace Center – Institute for Flight Mechanics.

Kreisselmeier, G., & Steinhauser, R. (1979). Systematic control design by optimizing a vector performance index. *IFAC Proceedings Volumes*, *12*(7), 113-117. (IFAC Symposium on computer Aided Design of Control Systems, Zurich, Switzerland, 29-31 August) doi: 10.1016/S1474-6670(17)65584-8

Morgado, J., & Sousa, J. (2009). O programa de investigação e tecnologia em veículos aéreos autónomos não tripulados da academia da força aérea. *IDN Cadernos*, *II Série*(4), 9-24. Retrieved from `https://www.idn.gov.pt/pt/publicacoes/idncadernos/Documents/2009/caderno4_II.pdf`

Raymer, D. P. (1992). *Aircraft design: A conceptual approach*. American Institute of Aeronautics and Astronautics, Inc.

Saaty, T. L., & Vargas, L. G. (2012). *Models, methods, concepts & applications of the analytic hierarchy process* (2nd ed.). Springer. doi: 10.1007/978-1-4614-3597-6

Silva, J. (2017). *Design and optimization of a wing structure for a uas class i 145 kg* (Master's thesis, Academia da Força Aérea, Sintra, Portugal). Retrieved from `http://hdl.handle.net/10400.26/23156`

Silva, P. (2021). *Projeto detalhado do sistema propulsivo para um veículo aéreo não tripulado com uma célula de combustível de hidrogénio* (Unpublished master's thesis). Academia da Força Aérea, Sintra, Portugal.

Sá, P. (2021). *Projeto detalhado estrutural de veículo aéreo não tripulado com uma célula de combustível de hidrogénio* (Unpublished master's thesis). Academia da Força Aérea, Sintra, Portugal.

Virtanen, P., Gommers, R., Oliphant, T. E., Haberland, M., Reddy, T., Cournapeau, D., ... SciPy 1.0 Contributors (2020). SciPy 1.0: Fundamental Algorithms for Scientific Computing in Python. *Nature Methods*, *17*, 261–272. doi: 10.1038/s41592-019-0686-2